



Comparison of wind turbine wake properties in non-uniform inflow predicted by different CFD rotor models

Troldborg, Niels; Zahle, Frederik; Sørensen, Niels N.; Réthoré, Pierre-Elouan

Publication date:
2012

[Link back to DTU Orbit](#)

Citation (APA):

Troldborg, N., Zahle, F., Sørensen, N. N., & Réthoré, P-E. (2012). Comparison of wind turbine wake properties in non-uniform inflow predicted by different CFD rotor models [Sound/Visual production (digital)]. The science of Making Torque from Wind 2012, Oldenburg, Germany, 09/10/2012, <http://www.forwind.de/makingtorque>

DTU Library

Technical Information Center of Denmark

General rights

Copyright and moral rights for the publications made accessible in the public portal are retained by the authors and/or other copyright owners and it is a condition of accessing publications that users recognise and abide by the legal requirements associated with these rights.

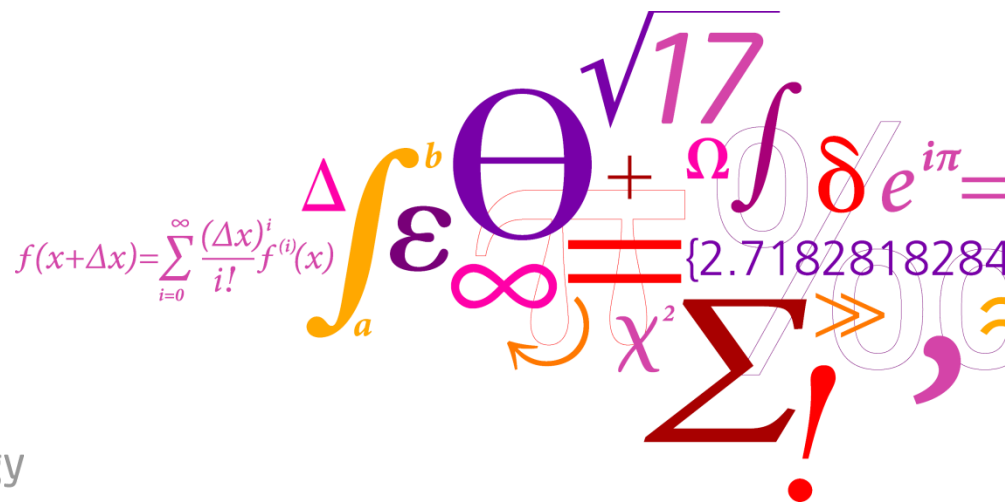
- Users may download and print one copy of any publication from the public portal for the purpose of private study or research.
- You may not further distribute the material or use it for any profit-making activity or commercial gain
- You may freely distribute the URL identifying the publication in the public portal

If you believe that this document breaches copyright please contact us providing details, and we will remove access to the work immediately and investigate your claim.

Comparison of wind turbine wake properties in non-uniform inflow predicted by different CFD rotor models

Niels Trolborg, Frederik Zahle, Niels N. Sørensen, Pierre-Elouan Réthoré

Wind Energy Department, DTU Wind Energy, DK-4000 Roskilde, Denmark



Background

Wind turbine models in CFD

- Fully resolved rotor (FR)
- Actuator line model (AL)
- Actuator disc model (AD)

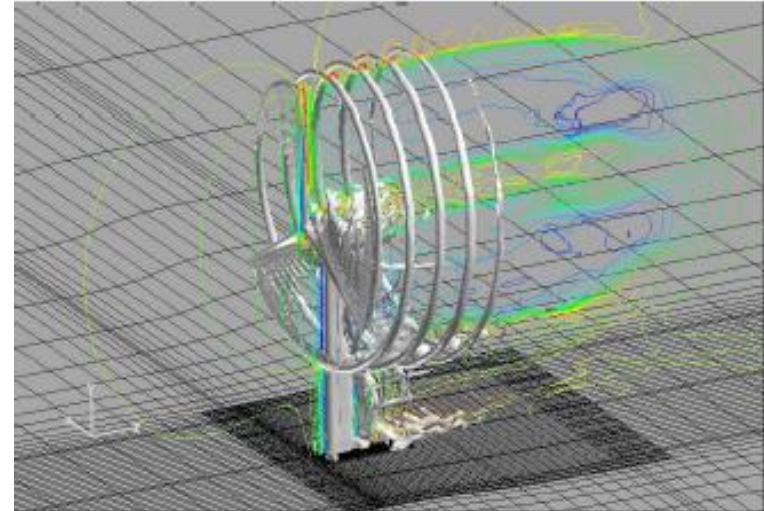
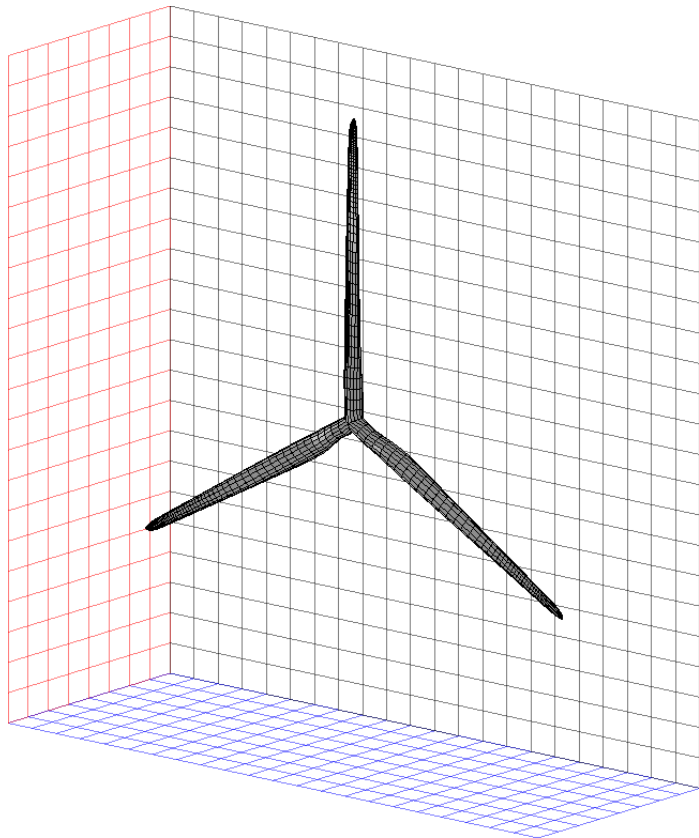


Background

Wind turbine models in CFD

- Fully resolved rotor (FR)
- Actuator line model (AL)
- Actuator disc model (AD)

- The blade/airfoil boundary layer is resolved
- The required number of grid points for one rotor using RANS is $O(10^7)$
- Provides detailed insight about flow behaviour
- Usually used for accurately predict loads and power production
- Too computationally heavy for several wind turbines.

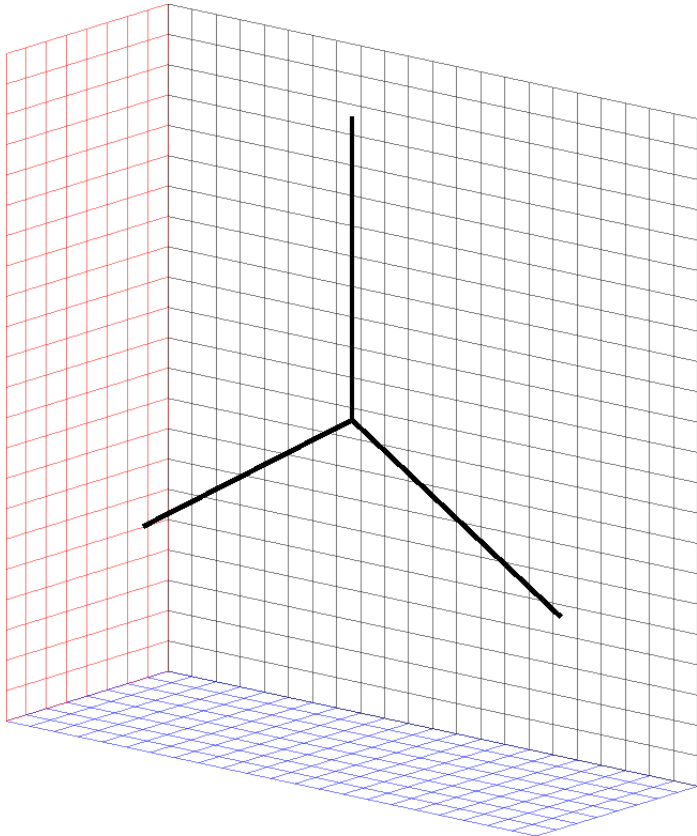


Background

Wind turbine models in CFD

- Fully resolved rotor (FR)
- Actuator line model (AL)
- Actuator disc model (AD)

➤ Blades represented as lines.

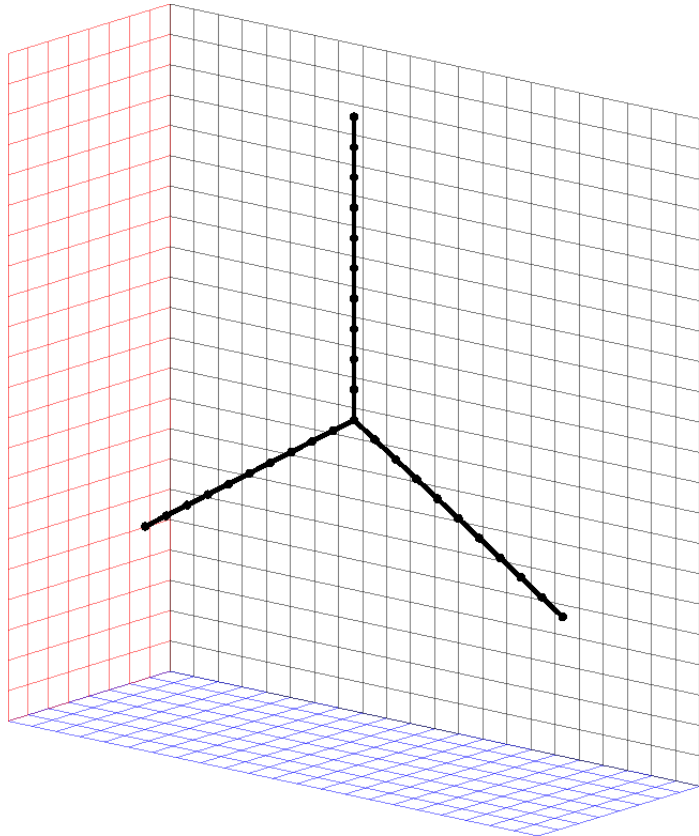


Background

Wind turbine models in CFD

- Fully resolved rotor (FR)
- Actuator line model (AL)
- Actuator disc model (AD)

- Blades represented as lines.
- Aerodynamic blade forces determined from 2D airfoil data.

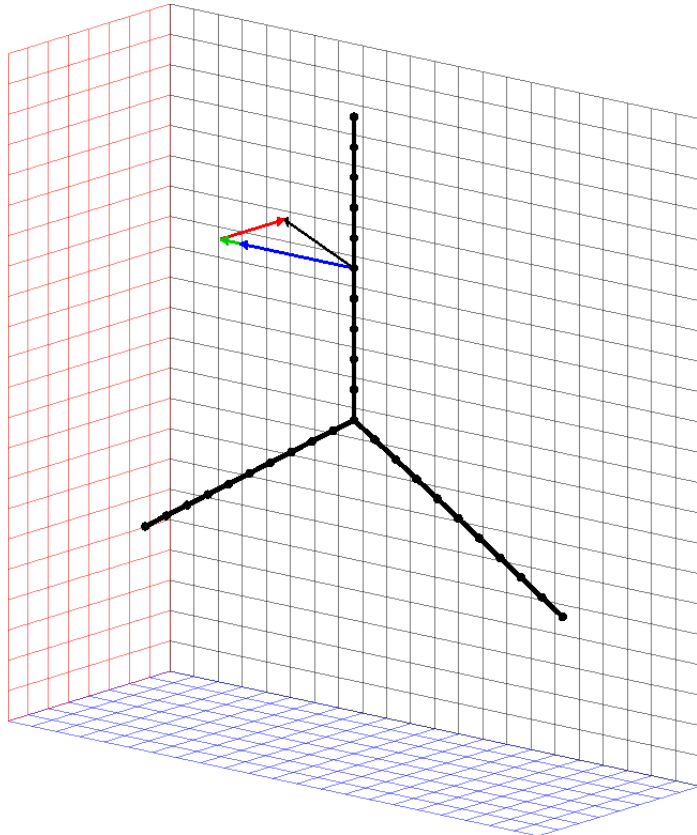


Background

Wind turbine models in CFD

- Fully resolved rotor (FR)
- Actuator line model (AL)
- Actuator disc model (AD)

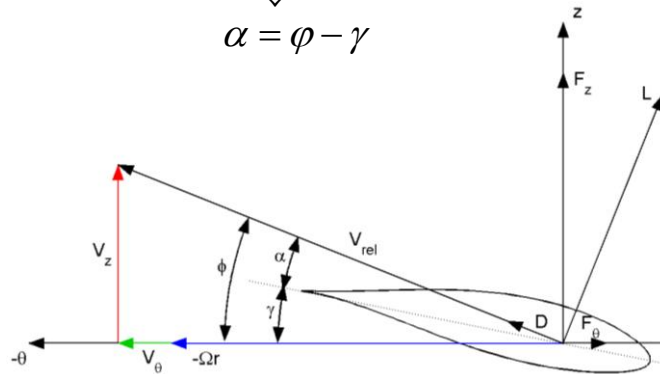
- Blades represented as lines.
- Aerodynamic blade forces determined from 2D airfoil data.



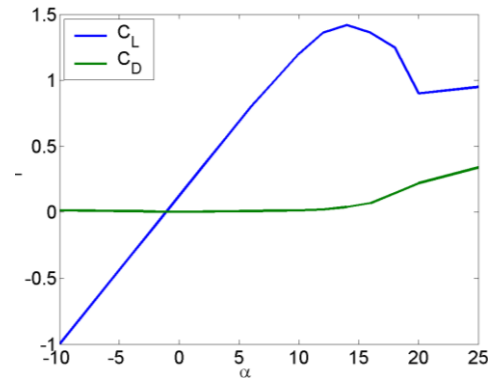
$$\varphi = \tan^{-1}\left(\frac{V_z}{\Omega r - V_\theta}\right)$$

$$\Downarrow$$

$$\alpha = \varphi - \gamma$$



$$\mathbf{f} = \begin{pmatrix} L \\ D \end{pmatrix} = \frac{1}{2} \rho V_{rel}^2 c \begin{pmatrix} C_L(\alpha) \mathbf{e}_L \\ C_D(\alpha) \mathbf{e}_D \end{pmatrix}$$



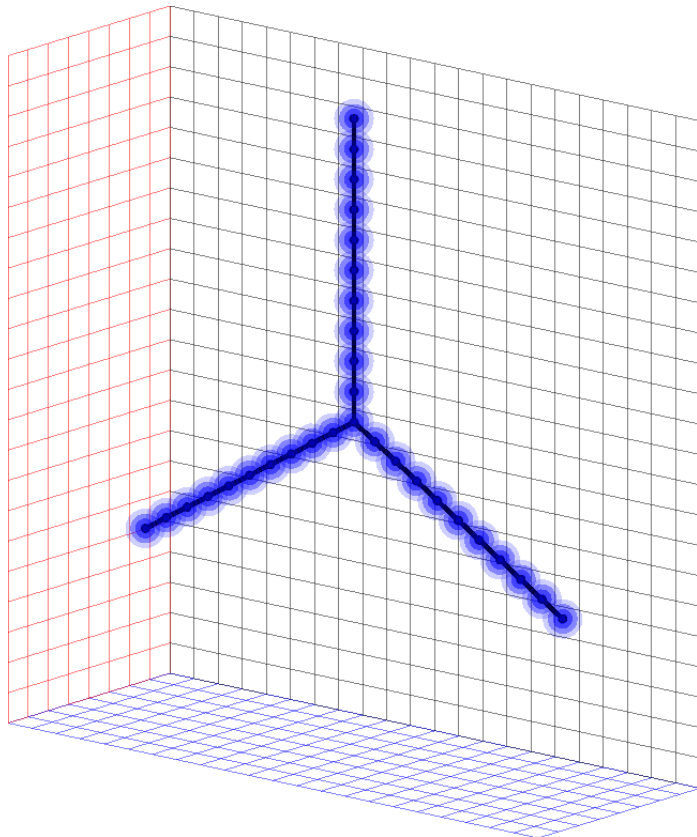
Background

Wind turbine models in CFD

- Fully resolved rotor (FR)
- Actuator line model (AL)
- Actuator disc model (AD)

- Blades represented as lines.
- Aerodynamic blade forces determined from 2D airfoil data.
- Blade forces smeared to avoid singular behaviour.

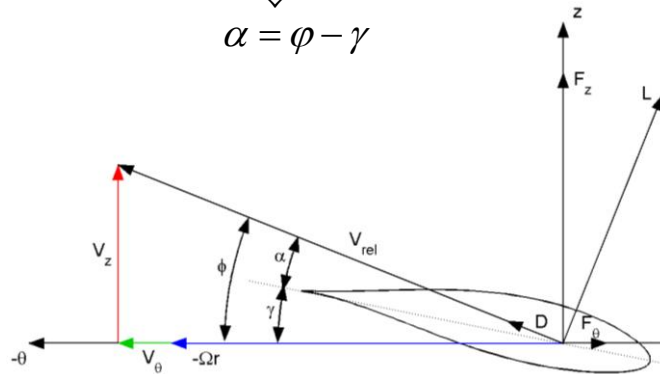
$$\mathbf{f}_\varepsilon = \mathbf{f} \otimes \eta_\varepsilon, \quad \eta_\varepsilon = \frac{1}{\varepsilon^3 \pi^{3/2}} \exp\left[-\frac{d^2}{\varepsilon^2}\right]$$



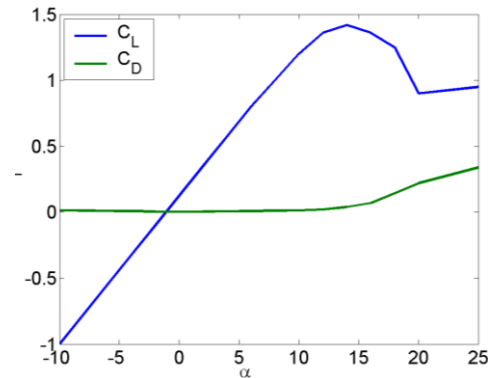
$$\varphi = \tan^{-1}\left(\frac{V_z}{\Omega r - V_\theta}\right)$$

$$\Downarrow$$

$$\alpha = \varphi - \gamma$$



$$\mathbf{f} = \begin{pmatrix} L \\ D \end{pmatrix} = \frac{1}{2} \rho V_{rel}^2 c \begin{pmatrix} C_L(\alpha) \mathbf{e}_L \\ C_D(\alpha) \mathbf{e}_D \end{pmatrix}$$



Wind turbine models in CFD

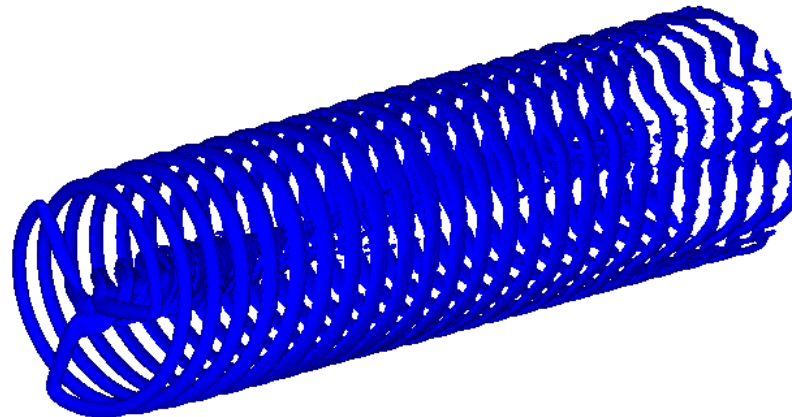
- Fully resolved rotor (FR)
- Actuator line model (AL)
- Actuator disc model (AD)

Advantages:

- Low number of grid points $O(10^6)$ needed compared to full rotor CFD.
- Applicable with simple grid geometries.
- Captures the most important features of the wake including tip/root vortices.
- Well suited for LES simulations (no boundary layers need to be resolved)

Disadvantages:

- Relies on airfoil data

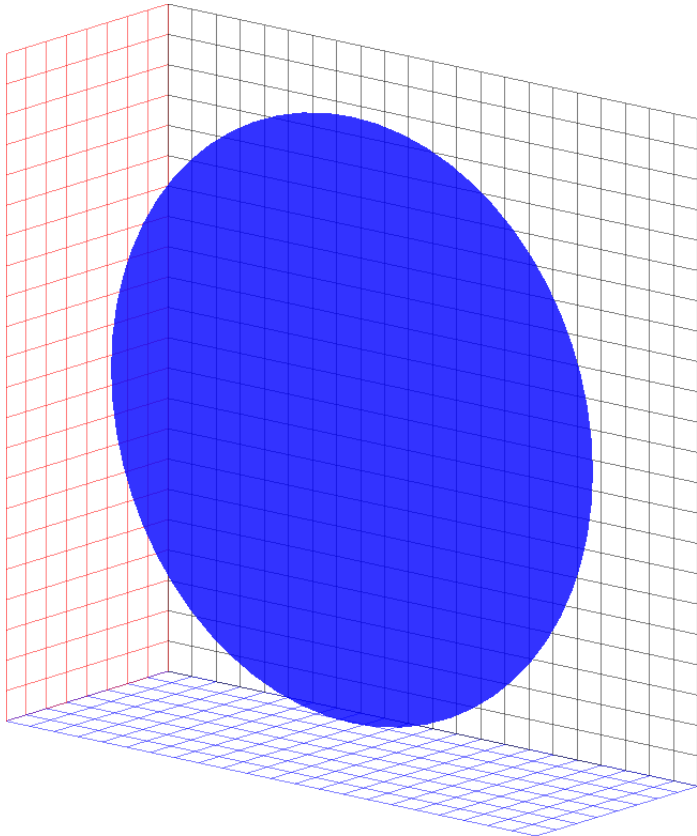


Background

Wind turbine models in CFD

- Fully resolved rotor (FR)
- Actuator line model (AL)
- Actuator disc model (AD)

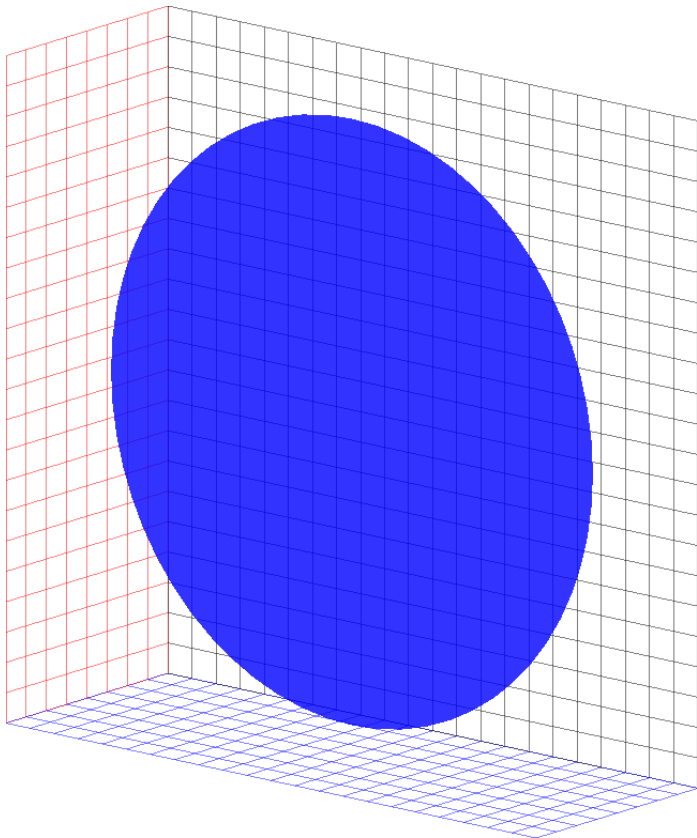
➤ Rotor represented by forces distributed on permeable disc.



Wind turbine models in CFD

- Fully resolved rotor (FR)
- Actuator line model (AL)
- Actuator disc model (AD)

- Rotor represented by forces distributed on permeable disc.
- The disc loading is either prescribed or determined from airfoil data.
- Pressure velocity decoupling avoided using Gaussian force smearing or a modified Rhie-Chow algorithm



Wind turbine models in CFD

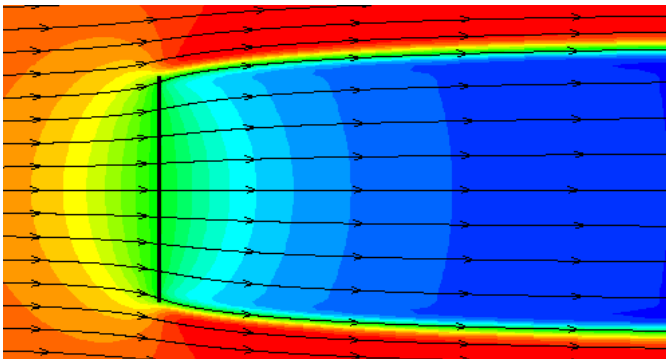
- Fully resolved rotor (FR)
- Actuator line model (AL)
- Actuator disc model (AD)

Advantages:

- Low number of grid points
- Applicable with simple grid geometries
- Well suited for LES simulations
- Large time steps can be used
- Can run in steady state

Disadvantages:

- Relies on airfoil data
- Does not capture influence of individual blades
- May be questionable in non-uniform inflow



Axial velocity contours and streamlines for a uniformly loaded disc at $C_T=0.89$

Summary:

- AL/AD typically used for wake studies
- Details of rotor geometry assumed unimportant in far wake

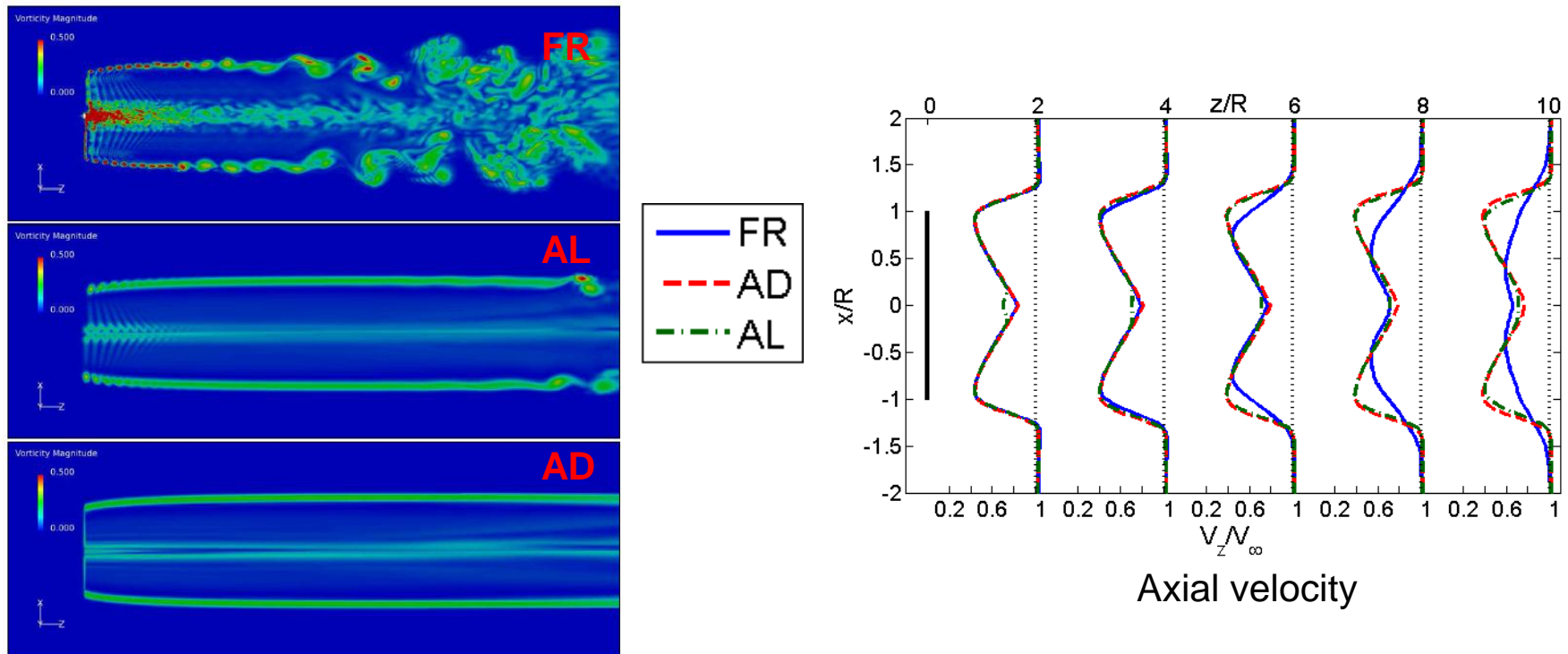
Objectives:

- Study importance of wind turbine model on wake characteristics
 - How much details are lost due to the simpler models?
- Conduct a consistent comparison of the three models
 - Same numerical setup for all models



Simulations of NREL 5MW reference turbine in non-sheared laminar inflow

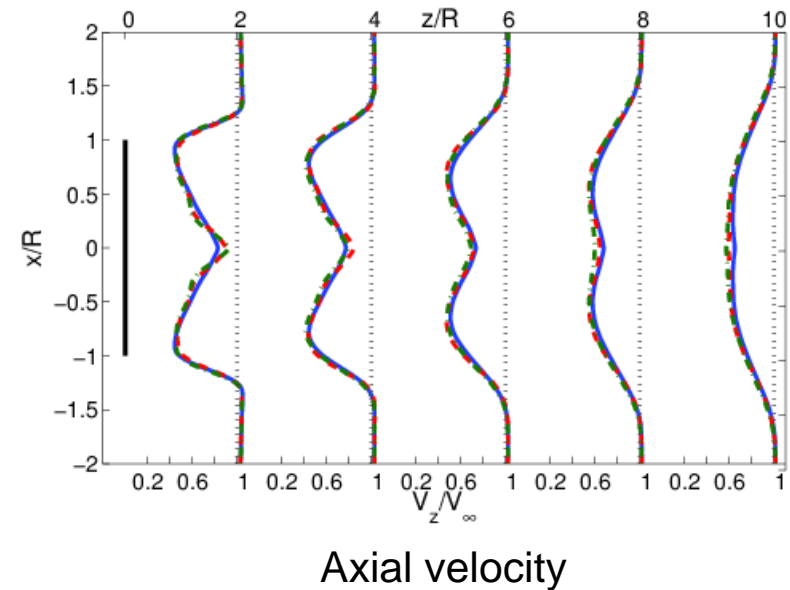
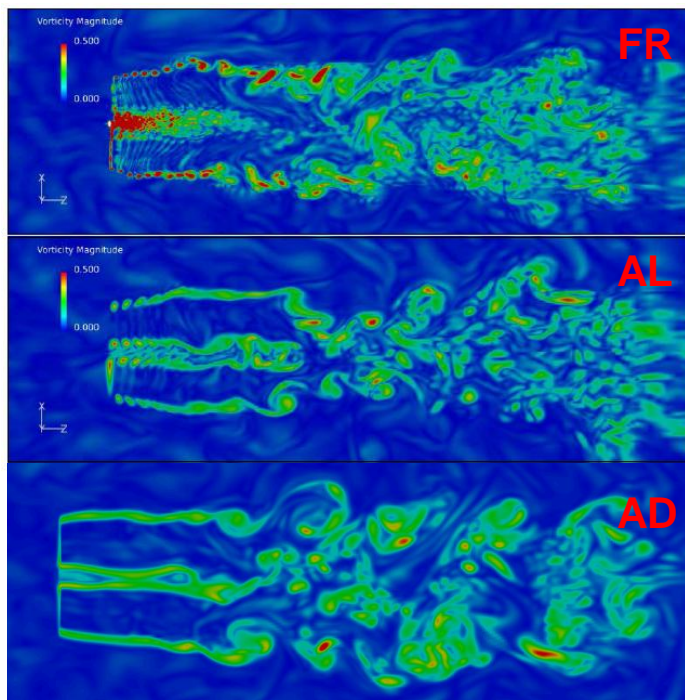
- Wake of FR develops faster into a bell shaped form than the AL and AD.
- Faster spreading of wake is caused by larger TKE in the FR simulation.



Snapshot of vorticity magnitude contours in horizontal cross-section through rotor center.

Previous work

Simulations of NREL 5MW reference turbine in non-sheared turbulent inflow



Snapshot of vorticity magnitude contours in horizontal cross-section through rotor center.

Objectives:

- Study importance of wind turbine model on wake characteristics in non-uniform inflow:
 - Sheared inflow
 - Yawed inflow
- Simulating the 2MW NM80 turbine using similar numerical setup



Approach – Flow solver

EllipSys3D:

- In-house CFD code
- Incompressible Navier-Stokes equations
- Finite volume discretization
- Structured curvilinear grids
- Pressure/Velocity formulation
- Multigrid
- Multiblock
- Grid sequencing
- MPI

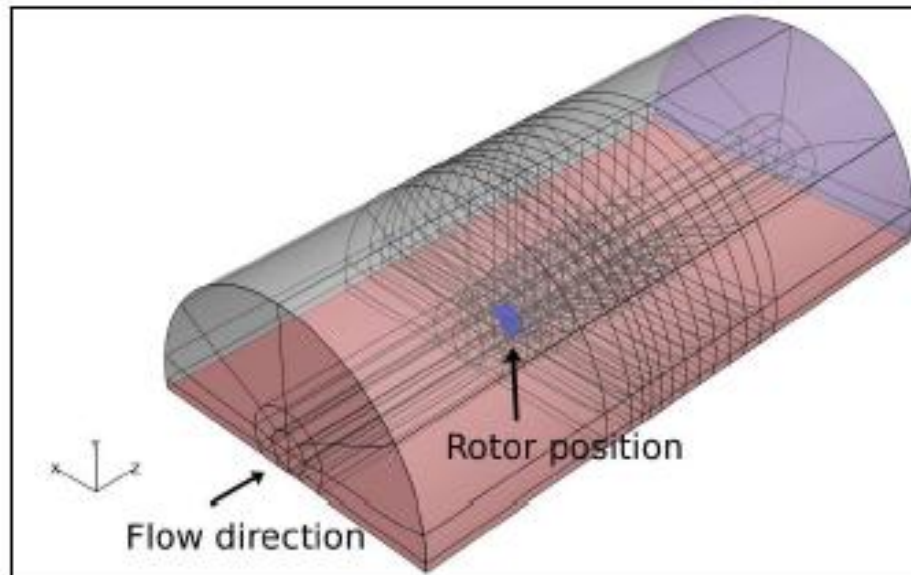
Solver parameters:

- QUICK/QUICK_CDS4
- SIMPLE
- DES

Approach - Numerical setup

Background mesh:

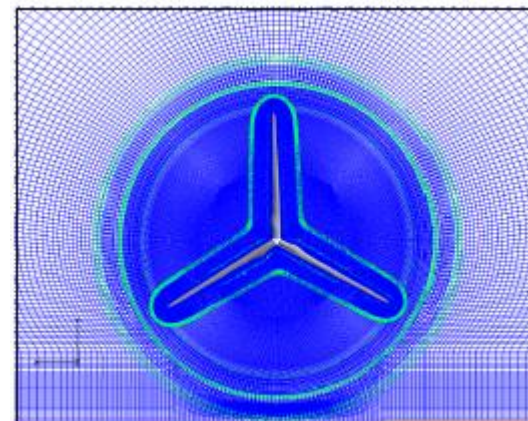
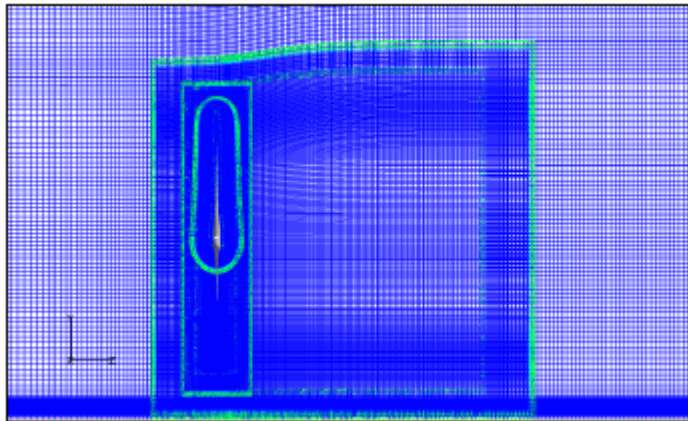
- Same background mesh for all simulations
- Half cylinder with radius $8D$
- 308 blocks of 32^3 ($10.1 \cdot 10^6$ cells)
- High resolution of the first $5D$ of the wake (cell size $1.3\text{m} \times 1.3\text{m} \times 0.8\text{m}$)



Approach - Numerical setup

Full rotor with overset grid:

- Four overlapping mesh groups
- Rotor mesh generated using HypGrid3D to form an O-O topology
- Total number of grid points is $26.7 \cdot 10^6$
- Rotor surface with a non-slip boundary condition
- First cell height $y=1.0 \cdot 10^6$ ($y^+ < 2$)



Approach - Numerical setup

Actuator line simulations:

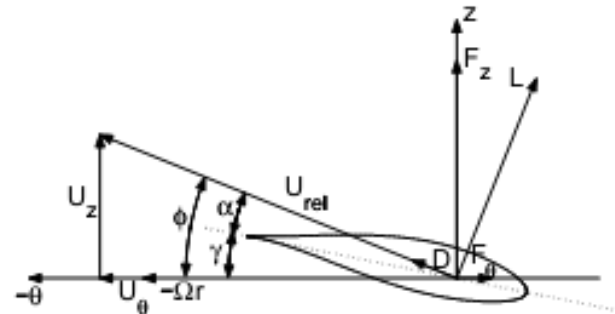
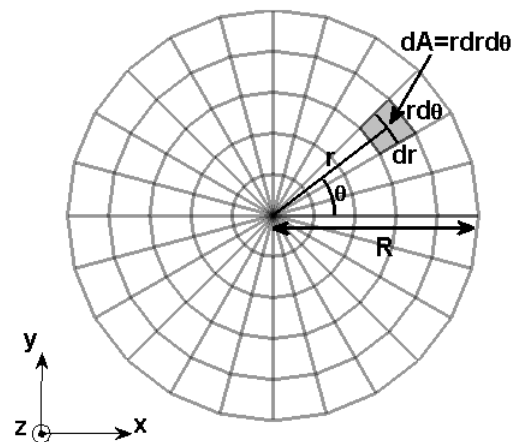
- Same background mesh as the full rotor simulation ($10.1 \cdot 10^6$ cells)
- Force smearing using 3D convolution
- 33 force elements along each line



Approach - Numerical setup

Actuator disc simulations:

- Same background mesh as the full rotor simulation ($10.1 \cdot 10^6$ cells)
- 33 radial force elements
- Force smearing using 1D convolution in normal and radial direction
- Forces on each differential area $dA=rdrd\theta$ is determined from local flow conditions and airfoil data.



Results

Test cases

- Sheared inflow
- Yawed inflow

Results

Test cases

- Sheared inflow
- Yawed inflow

➤ $V_\infty = 8 \text{ m/s}$

➤ Power law inflow ($\alpha = 0.55$):

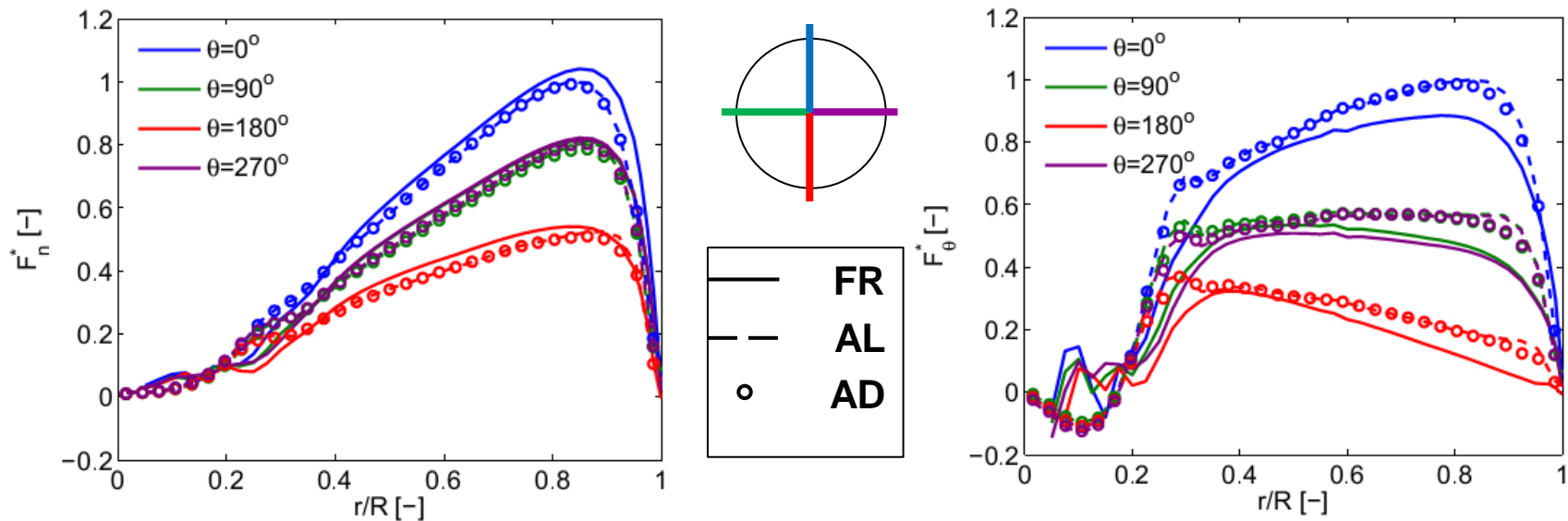
$$V_z = V_\infty \left(\frac{y}{H} \right)^\alpha$$

Results

Test cases

- Sheared inflow
- Yawed inflow

- Normal loads in good agreement
- Tangential loads less in FR than in AL and AD



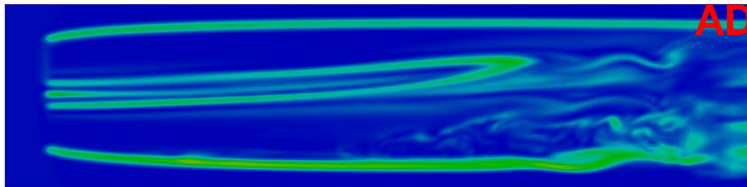
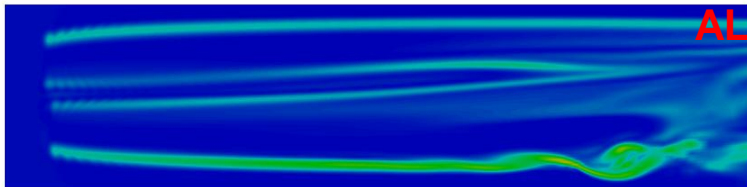
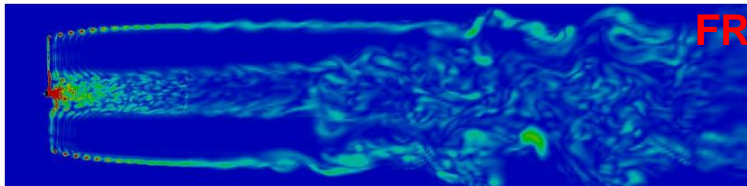
Spanwise distribution of normal and tangential loads at various azimuth positions

Results

Test cases

- Sheared inflow
- Yawed inflow

- Vorticity from tip vortices much stronger in FR than in AL and AD.
- Wake of FR more unstable
- Similar vorticity contours for AL and AD (except for instability in the far wake)
- Reasons for more unstable wake of FR:
 - Higher grid resolution
 - Fluctuating loads (e.g. stall effects near root)



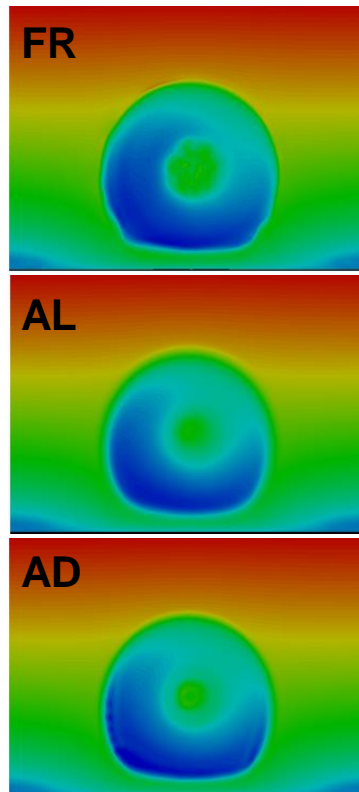
Snapshot of vorticity magnitude contours in horizontal cross-section through rotor center.

Results

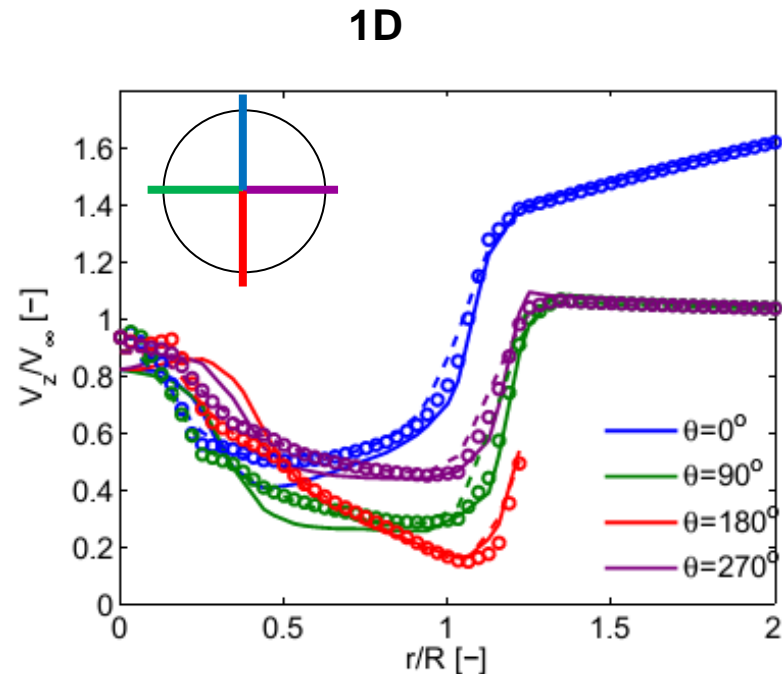
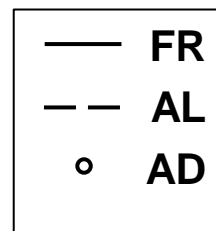
Test cases

- Sheared inflow
- Yawed inflow

- Good agreement in predicted near wake deficit
- AL and AD in close agreement
- Wake of FR develops faster into a bell shaped form than the AL and AD.



Streamwise velocity contours in cross-section 1D downstream.



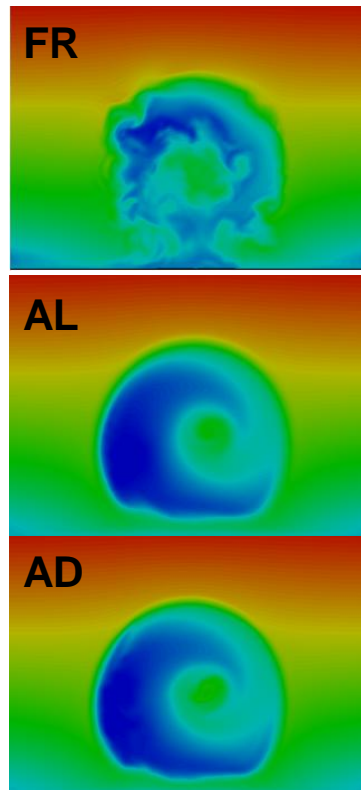
Mean streamwise velocity 1D downstream for various azimuth positions

Results

Test cases

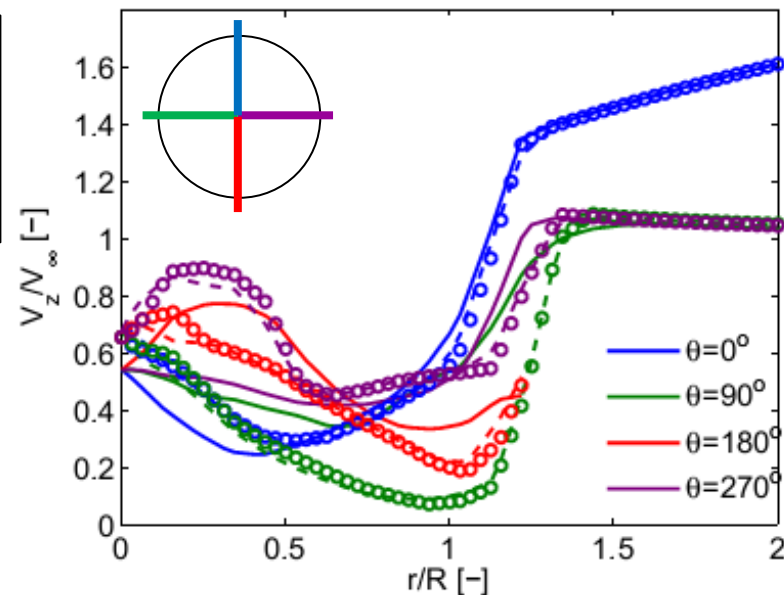
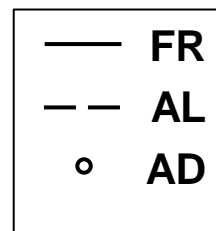
- Sheared inflow
- Yawed inflow

- Good agreement in predicted near wake deficit
- AL and AD in close agreement
- Wake of FR develops faster into a bell shaped form than the AL and AD.



Streamwise velocity contours in cross-section 3D downstream.

3D



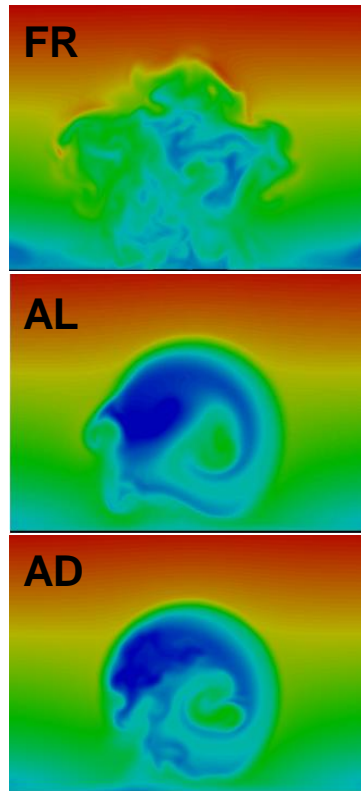
Mean streamwise velocity 3D downstream for various azimuth positions

Results

Test cases

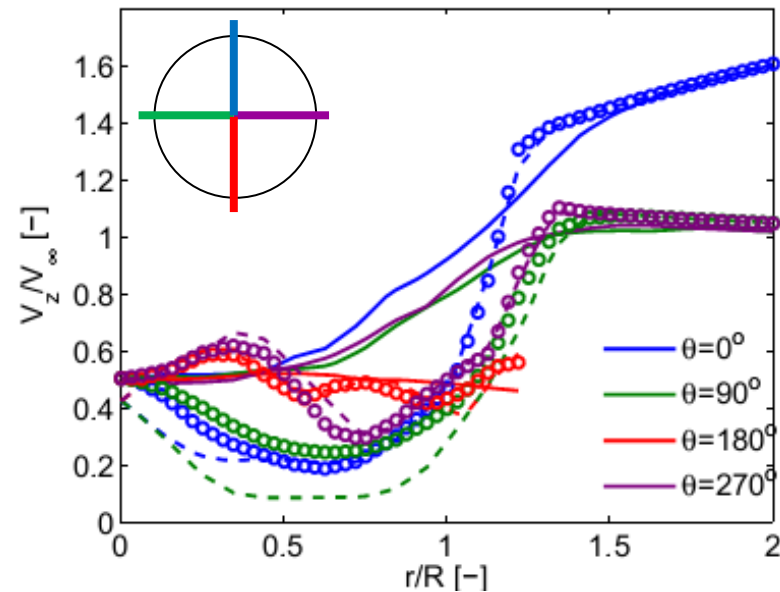
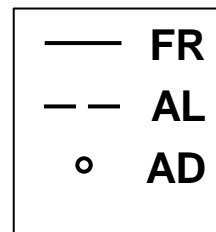
- Sheared inflow
- Yawed inflow

- Good agreement in predicted near wake deficit
- AL and AD in close agreement
- Wake of FR develops faster into a bell shaped form than the AL and AD.



Streamwise velocity contours in cross-section 5D downstream.

5D



Mean streamwise velocity 5D downstream for various azimuth positions

Results

Test cases

- Sheared inflow
- Yawed inflow

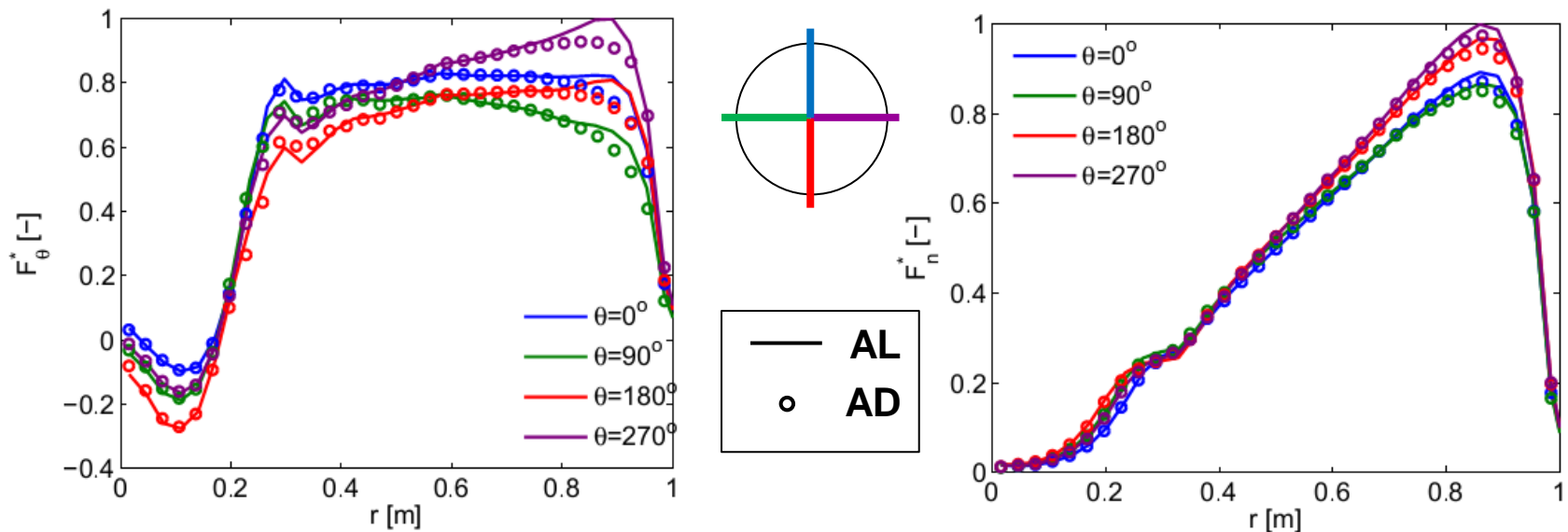
- $V_{\infty} = 8 \text{ m/s}$
- Yaw error of 20°

Results

Test cases

- Sheared inflow
- Yawed inflow

➤ Load predictions in good agreement



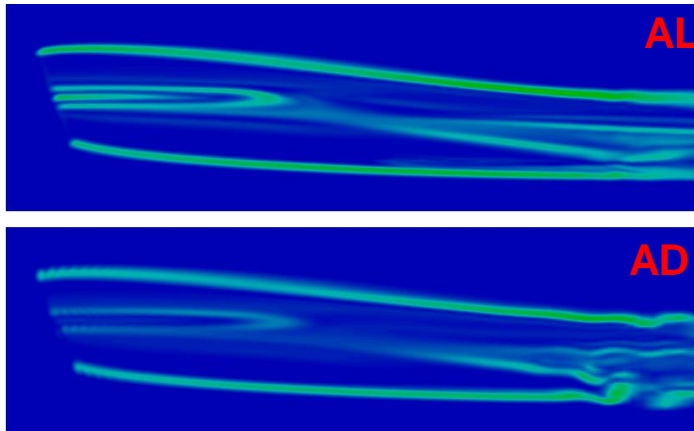
Spanwise distribution of normal and tangential loads at various azimuth positions

Results

Test cases

- Sheared inflow
- Yawed inflow

➤ Similar vorticity contours



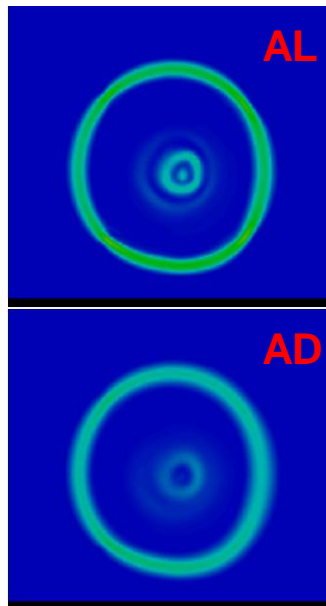
Snapshot of vorticity magnitude contours in horizontal cross-section through rotor center.

Results

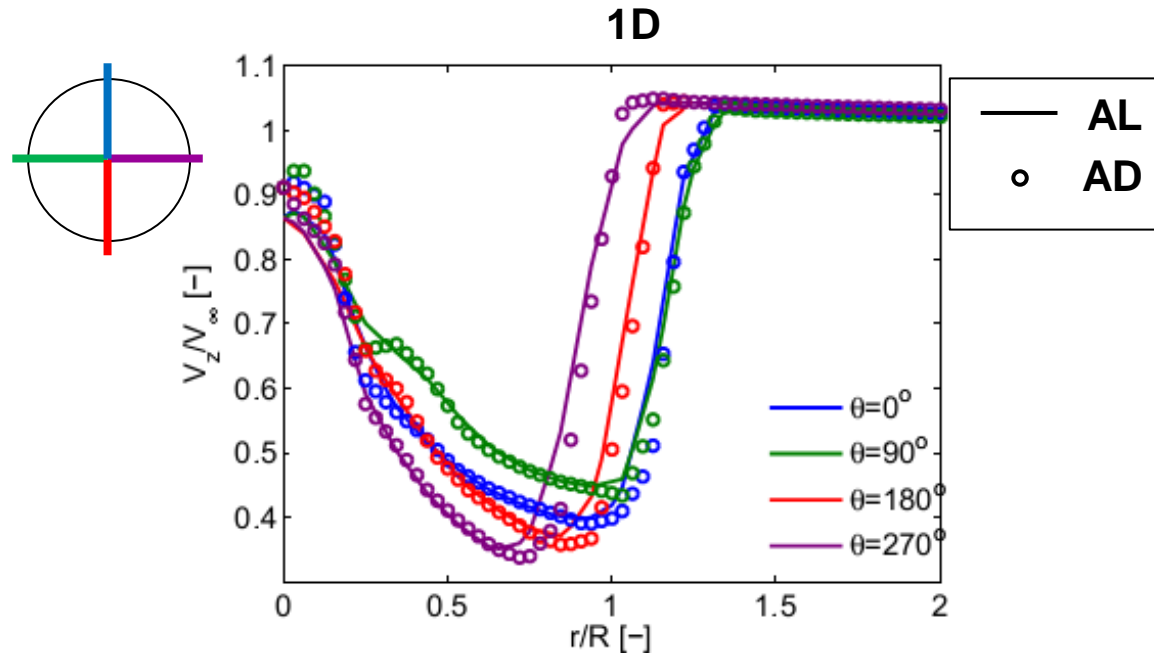
Test cases

- Sheared inflow
- Yawed inflow

➤ Good agreement in predicted wake deficit and wake structure



Vorticity magnitude contours in cross-section 1D downstream.



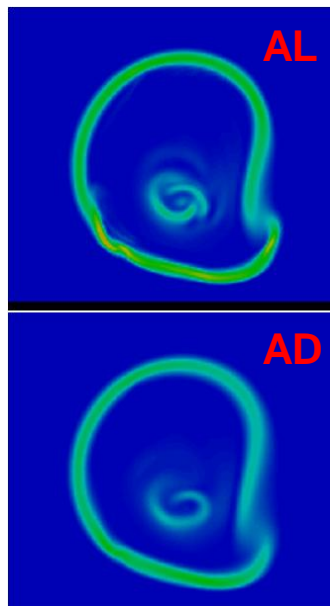
Mean streamwise velocity 1D downstream for various azimuth positions

Results

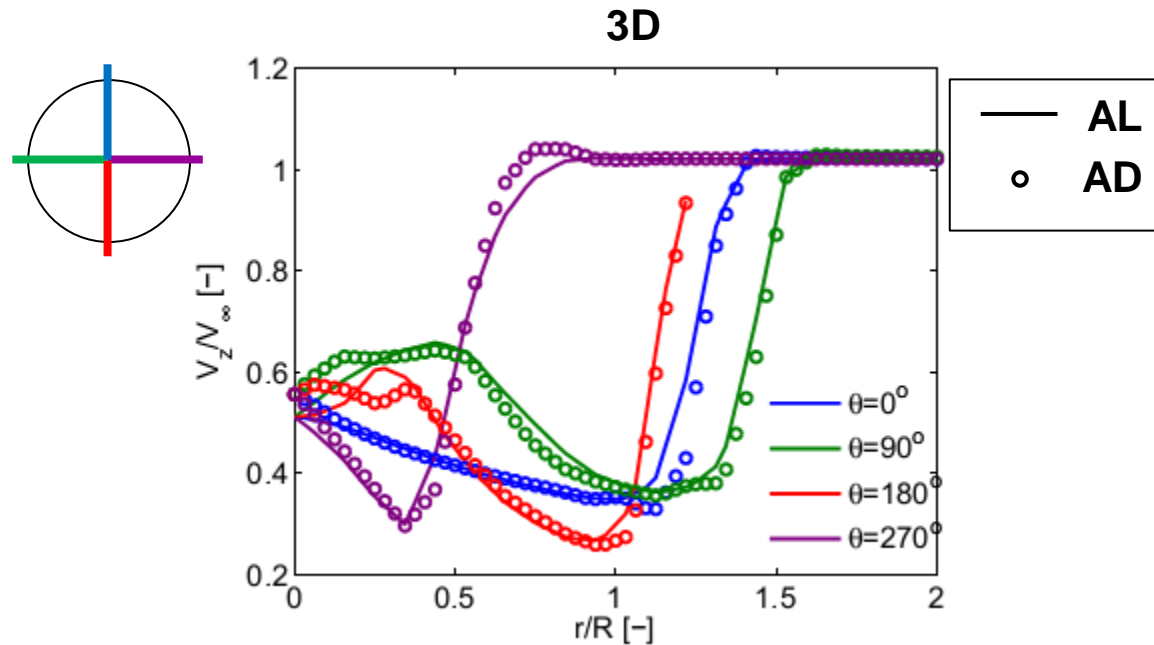
Test cases

- Sheared inflow
- Yawed inflow

➤ Good agreement in predicted wake deficit and wake structure



Vorticity magnitude contours in cross-section 3D downstream.



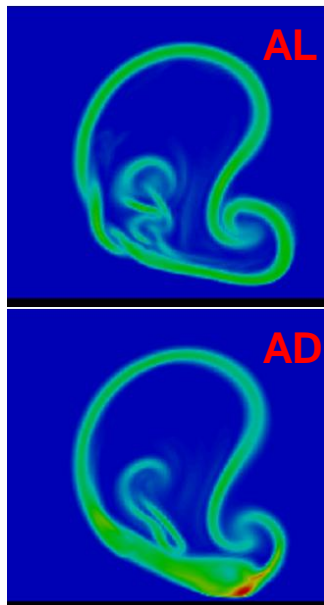
Mean streamwise velocity 3D downstream for various azimuth positions

Results

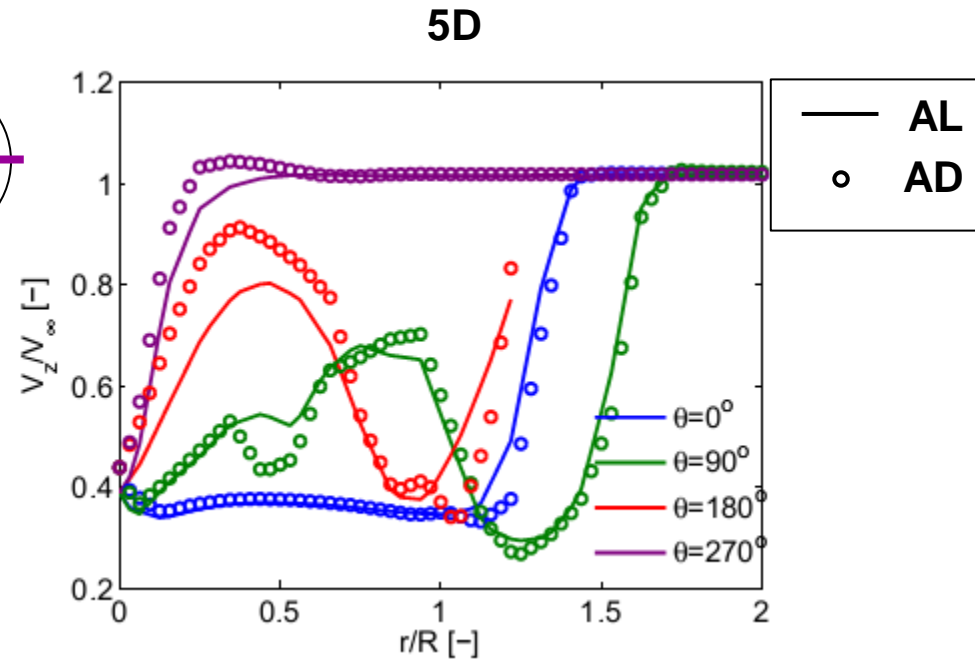
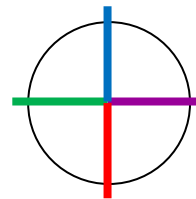
Test cases

- Sheared inflow
- Yawed inflow

➤ Good agreement in predicted wake deficit and wake structure



Vorticity magnitude contours in cross-section 5D downstream.



Mean streamwise velocity 5D downstream for various azimuth positions

- Sheared inflow
 - Three models show good agreement in axial velocity up to 2D downstream of the turbine.
 - Further downstream the FR simulation predicts a faster smearing of the mean gradients
 - Much higher turbulence in the FR simulation
 - Generally good agreement between AL and AD for all downstream position.

- Yawed inflow
 - Good resemblance between wake behavior predicted using AL and AD.
 - AD representation as accurate as AL even in non-uniform inflow.